Conf-9206195-

BNL-47974

INVERSE FREE ELECTRON LASER ACCELERATOR

A. Fisher, J. Gallardo, J. Sandweiss, A. van Steenbergen

September 1992

NATIONAL SYNCHROTRON LIGHT SOURCE

BROOKHAVEN NATIONAL LABORATORY
ASSOCIATED UNIVERSITIES, INC.

Under Contract No DE-AC02-76CH00016 with the
UNITED STATES DEPARTMENT OF ENERGY

Submitted to the Third Workshop on Advanced Accelerator Concepts,
Port Jefferson, NY, June 14-20, 1992.

INVERSE FREE ELECTRON LASER ACCELERATOR*

A. Fisher, J. Gallardo, J. Sandweiss**, A. van Steenbergen
National Synchrotron Light Source and Physics Department
Brookhaven National Laboratory, Upton, NY 11973

BNL--47974
DE93 001963

ABSTRACT

The study of the INVERSE FREE ELECTRON LASER, as a potential mode of electron acceleration, is being pursued at Brookhaven National Laboratory. Recent studies have focussed on the development of a low energy, high gradient, multi stage linear accelerator. The elementary ingredients for the IFEL interaction are the 50 MeV Linac e^- beam and the 10^{11} Watt CO_2 laser beam of BNL's Accelerator Test Facility (ATF), Center for Accelerator Physics (CAP) and a wiggler. The latter element is designed as a fast excitation unit making use of alternating stacks of Vanadium Permendur (VaP) ferromagnetic laminations, periodically interspersed with conductive, nonmagnetic laminations, which act as eddy current induced field reflectors. Wiggler parameters and field distribution data will be presented for a prototype wiggler in a constant period and in a $\approx$ 1.5%/cm tapered period configuration.

The CO_2 laser beam will be transported through the IFEL interaction region by means of a low loss, dielectric coated, rectangular waveguide. Short waveguide test sections have been constructed and have been tested using a low power cw CO_2 laser. Preliminary results of guide attenuation and mode selectivity will be given, together with a discussion of the optical issues for the IFEL accelerator.

The IFEL design is supported by the development and use of 1D and 3D simulation programs. The results of simulation computations, including also wiggler errors, for a single module accelerator and for a multi-module accelerator will be presented.

I. INTRODUCTION

The study of the Inverse Free Electron Laser (IFEL) as a potential mode for particle acceleration, has been pursued at Brookhaven National Laboratory for a number of years now.[1-4] More recent studies have focussed on the development of a low energy (few GeV) multistage linear accelerator.[5] Specifically also, the design of a short accelerator module has been pursued, which would make use of the ATF high brightness, 50 MeV, Linac beam and its high power, 10^{11} Watt, CO_2 laser beam. This would be used to carry out an accelerator demonstration stage experiment[6] with such parameters as to be of potential interest towards the further development of a "competitive" high gradient electron Linac with a wavelength

*Work performed under the auspices of the U.S. Department of Energy, under Contract No. DE-AC02-76CH00016.
**Yale University

parameter of 10 μm, based on the IFEL principle, for maximum operating energies of up to a few GeV.

In the IFEL accelerator, the electron beam is accelerated by the interaction with the laser radiation wave in the medium of a periodic wiggler field. The theoretical description of the interaction has been given by a number of authors. Here, in Section II, in order to simplify the parameterization for a single module IFEL accelerator stage, use is made of the basic formalism describing the IFEL accelerator as given by CPZ[3], with the further assumption that electron energy loss effects due to synchrotron radiation emission is taken to be zero and that the laser beam attenuation due to absorption by the accelerating electrons is negligible. The latter assumption is abandoned in further detailed treatment here and, in Section VI, following KMR[7], a self consistent system of Lorentz equations for the electrons and the wave equations for the input laser field is used, to form the basis of both a 1-D and 3-D IFEL simulation program.

As will be detailed in Section II, for the IFEL accelerator, maximum rate of acceleration is achieved with the use of the highest magnetic field, tapered period length wiggler, hence, substantial effort has been devoted to the design of a matched to the purpose, high field, variable period, fast excitation wiggler.[8-10] This is presented in Section III.

A limitation of the IFEL accelerator rate of acceleration is due to the varying E field magnitude with distance in a diffraction limited laser, free space, transport mode. Making use of a relatively short wiggler section (e.g. $\approx$ 0.6 m) it is possible to keep the Rayleigh length (defined as the distance over which the cross sectional area of a "Gaussian" laser beam doubles in value) to a small value (e.g. $\approx$ 0.3 m) thereby enhancing the effective use of the available laser power [$E_L \propto \sqrt{(W/R)}$, where W = laser power, R = Rayleigh length; for a diffraction limited beam]. A disadvantage of this mode of laser transport is, however, that use must be made of periodically placed optical elements in a multistage accelerator system. Although this approach was studied in some detail and a possible conceptual approach was obtained[11] which preserved macroscopic synchronization of the electron bunches and the photon bunches in a multistage system, it was abandoned because of inherent complexity and difficulty in maintaining phase slip tolerances. Instead, the alternative of confinement of the laser radiation in a hollow optical waveguide has been adopted. As a matter of fact, the electron beam pipe passing through the IFEL wiggler acts as a (overmoded) wave guide for the CO_2 laser radiation taking into account the relative magnitudes of the CO_2 laser wavelength and gap magnitude of the IFEL wiggler. In general, attenuation of CO_2 light in metallic guides can be significant for a long accelerator. The use of dielectric coated guides[12] can reduce the attenuation leading to calculated attenuation coefficients of 10^{-5} dB/m.

A description of square aperture, dielectric coated guides is given in Section III, together with early results of CO_2 laser attenuation measurements of both dielectric coated guide sections and uncoated comparable stainless steel guide sections.

The use of an overmoded metallic guide brings with it problems of mode coupling, matching of phase and group velocity and parasitic mode contamination. These optical issues are addressed in Section V.

As indicated above, for early parameterization of a single IFEL module, a 1-D simulation code was used to model the acceleration process. Subsequent to this, a 3-D code was further developed and adopted, specifically also to study transverse and longitudinal phase space distributions of the IFEL accelerator. Results from IFEL simulation computations are presented in Section VI. With the availability of these two programs, the parameterization of a multimodule IFEL accelerator was carried out together with the adoption of a sensible error spectrum, with the aim of not only gaining insight into the achievable parameters for a multimodule IFEL system, but also to optimize further the single first module for the accelerator demonstration stage. This is discussed in Section VII.

II. IFEL ACCELERATOR EXPERIMENT

From CPZ[3], for the case of zero synchrotron radiation emission and negligible attenuation of the laser beam due to energy transfer to the electron beam, the relevant IFEL accelerator equations are given by:

$$\left(\frac{d\gamma}{dz}\right) = \xi_n A \frac{K}{\gamma} \sin\psi$$

$$\left(\frac{d\psi}{dz}\right) = \kappa - [k/(2n\gamma^2)]\,(1 + \eta K^2 + K_L^2 + 2\eta^{1/2}\xi_n K K_L \cos\psi) \quad , \quad with$$

$$A = \left(\frac{e E_L}{m_o c^2}\right),$$

and E_L the electric field of the laser EM wave; $\xi_n = F_n$ for a planar wiggler. The F_n function (n = harmonic number) is given by (n = 1,3,5, ...):
$F_n = 1/2\ \{J_{n-1}(x) - J_n(x)\}$ with $x = kK^2/8\kappa\gamma^2$ and J_i are Bessel functions.
Further: $K = eB\lambda_o/2\pi m_o c^2 = 93.4\ B\lambda_o$ [T.m.] with λ_o the wiggler period length, and

$$K_L = \frac{eE_L\lambda}{2\pi m_o c^2}$$

$\eta = 1$, helical wiggler; $\eta = 1/2$ planar wiggler
Ψ = phase of the electron oscillation relative to the EM wave as seen by the electron.
$\Psi = (k + \kappa)\, z - \omega t$; $\omega = kc = (2\pi/\lambda)c$; $\kappa = 2\pi/\lambda_o$.

For electron acceleration it is necessary that $\Psi \approx$ constant, or $(d\Psi/dt) = 0$, from which the resonant condition follows as:

$$\kappa = \frac{k}{2n\gamma^2}(1 + \eta K^2) \quad for \quad K_L < K$$

or, for K >> 1: $\lambda = (\eta\lambda_o K^2)/(2n\gamma^2)$.

With the synchronism condition, for a fixed value of λ, there remains one arbitrary function in the equations with which to optimize the accelerator, i.e. equivalent sets of accelerator parameter equations may be obtained for the case whereby either

$$\lambda_o(z) \quad or \quad B(z) \quad or \quad K(z) \; \alpha \; B(z).\lambda_o(z)$$

is adopted as an arbitrary function in the equations. These equivalent sets of equations are given in Table I, where the rate of acceleration, $(d\gamma/dz)$, is given as a function of either $\lambda_o(z)$, $(\Omega/\omega) = C_1\lambda B(z)$ or K(z). In actual execution of designing an IFEL accelerator structure, limiting parameters are introduced by the maximum wiggler field value and minimum wiggler period length value. In effect, it is evident from the equations given in Table I that for a $\lambda_o(z)$ = const. accelerator, the maximum wiggler B value is encountered at the exit of the accelerator, but for a K(z) = const. accelerator the maximum wiggler field magnitude is encountered at the injection end of the accelerator. In general, it can be shown[5] that for an IFEL accelerator, for which the synchrotron radiation loss term is negligible, and which has been optimized to the limit of the maximum wiggler field anywhere in the structure, the maximum rate of acceleration, averaged over the full accelerator structure length, is obtained for the case of a B(z) = const. accelerator. This is further shown in Fig. 1 for the specific case of a 1 GeV IFEL accelerator for which a maximum (pulsed excitation) field value of 1.5 Tesla is adopted.

For the demonstration stage accelerator the parameters are developed based on the use of a constant maximum wiggler field magnitude of B = 1.25 T. The minimum value of the wiggler period length, in this case, with an injection energy of 50 MeV, is 2.87 cm (n = 1) which, taking a wiggler gap value of 0.4 cm into account, is technically acceptable. Recall also, however that in this case $\lambda_o \; \alpha \; n^{1/3} \; \gamma^{2/3}$, and that the harmonic mode of acceleration, n = 3,5... could be employed in a short, low energy front end section, of the accelerator.

For the constant B accelerator structure, with an adopted value of B_{max} = 1.25 T and n = 1, to first order, the magnitudes of $\lambda_o(z)$, K(z) and $(d\gamma/dz)$ are given by

$$\lambda_o = 0.0014 \; \gamma^{2/3} \quad , \quad K = 0.167 \; \gamma^{2/3} \; , \quad \frac{1}{A}\left(\frac{d\gamma}{dz}\right) = 0.167 \; \gamma^{-1/3} \; F_1$$

with $A = A \sin\Psi$. The latter equation may be integrated to yield:

$$E(z) = \left[\frac{4}{3}(F_E \cdot 10^4)\left(\frac{2}{\eta}\right)^{1/3}(\xi \sin\psi)\left(\frac{\Omega}{\omega}\right)^{1/3}(m_o c^2)^{1/3} z + E^{4/3}(z=0)\right]^{3/4}$$

with $eE_O = F_E \cdot 10^4$ [MeV/m]; z[m]; $\xi = F_1$, and $F_E = (W_L/2 \; 10^{11})^{1/2}$.

For the case of the low loss waveguide CO_2 laser transport, the laser field magnitude follows from:

$$W = \left(\frac{1}{4Z_o}\right) \iint E_l^2(0,0) \cos\left(\frac{\pi x}{2D}\right) \cos\left(\frac{\pi y}{2D}\right) dxdy = \left(\frac{D^2}{4Z_o}\right)\left(\frac{16}{\pi^2}\right) E_l^2(0,0) \text{ , where}$$

D is the half transverse aperture of the guide (1.4 mm). Hence, for a laser power of W = 2.10^{11} Watts, a field magnitude of $E_\ell \approx 10^4$ MV/m is obtained.

The design parameters for an IFEL demonstration stage accelerator, with accelerator section length of 0.6 m can now be derived straightforwardly. An example of a self consistent set of parameters is tabulated in Table II. Energy and wiggler period length, as a function of distance are graphically given in Fig. 2. As is evident, with injection energy of E_i = 50 MeV, approximately a doubling of energy is achieved in a sector length of 0.6 m, i.e. with a given laser power of W = 2 x 10^{11} Watts and E field loss factor of α = 0.025 ($E(z) = E_o \exp -\alpha z$) a mean accelerator field magnitude of ~ 90 MV/m may be achieved. The effectiveness of the IFEL accelerator, with the cited parameters, is further illustrated in Fig. 3 where the particle distribution in longitudinal phase space is shown at the exit of the IFEL module and where the population distribution is shown versus energy. Particle trapping in an accelerating "bucket" with explicit momentum separation of accelerated and non accelerated electrons is clearly in evidence.

Responding to the challenge posed during the Port Jefferson workshop (June 14-20, 1992), the parameters for a 100 MeV IFEL accelerator were derived based on projected near-term anticipated parameters for the electron beam and the CO_2 laser beam of the BNL ATF/CAP facility, i.e. laser parameters, W = 10^{11} Watts, Δt = 10 psec, J = 1 Joule; and e^- beam parameters, E = 50 MeV, I = 5 mA, $(\Delta E/E) = \pm 3\ 10^{-3}$, emittances 7 10^{-8} rad.m. With these parameters, in order to achieve an energy gain of 100 MeV, four accelerator modules similar to that enumerated in Table I are required. This is further shown in Fig. 4 where a four module test configuration is given. Evidently, with this relatively modest laser power a mean accelerating gradient of approximately 50 MeV/m is achievable.

III. FAST EXCITATION VARIABLE PERIOD WIGGLER

The IFEL electron accelerator as parameterized here makes use of a quasi-sinusoidal magnetic field, with constant maximum field amplitude, and varying wiggler period length. Related to the beam injection energy into the IFEL linear accelerator, this period length may vary from a few cm's in length to larger period length magnitudes. Such a structure could possibly be constructed using presently known techniques employing permanent magnet material. It would, however, be very high in cost because of the nonrepeat feature of the wiggler period length. Hence, for the present objective, a new design approach has been pursued, which makes use of easily stackable, geometrically alternating substacks of identical ferromagnetic material (Vanadium Permendur) laminations, which is driven in a fast excitation mode, and which makes use of interleaving of conductive, nonmagnetic, laminations, which act as eddy current induced "field reflectors".[8-10]

For the ferromagnetic laminations for this wiggler design a number of basic configurations have been studied by means of two dimensional mesh computations (POISSON) and by means of actual short wiggler model measurements. The adopted configuration is illustrated in Fig. 5. As shown, the magnetic material laminations are assembled in ($\lambda_o/4$) thickness substacks, and separated by nonmagnetic material laminations. Four straight current conductors, parallel to the axis of the composite assembly and interconnected only at the ends of the total assembly, constitute the current single excitation loop for the wiggler, permitting ease of stack assembly, compression of the stacks by simple tie rods, and ready adoption of either constant period length or sequentially varying period length.

Subsequent to early trials of a fast excitation driven wiggler, the use of eddy current induced "field reflectors" in the laminated wiggler core, was initiated, as also indicated in Fig. 5. This led to dramatic enhancement of maximum on axis field magnitude, for a specific wiggler period length and gap value, as shown by the experimental data given in Fig. 6. Field saturation is evident in these results for higher excitation current values. The onset of field saturation is clearly discernible with the onset of distortion of the magnetic measurement probe voltage versus time display. The field value corresponding to the onset of saturation, for a sequence of model measurements with different period length values, was obtained, both for the case of wiggler models without field reflection and with field reflection. This is summarized in Fig. 7. As is evident from these results the specification of 12.5 kG, for a 2.9 cm period length wiggler, with gap value of 4 mm, can readily be met for the fast excitation wiggler with field reflection.

The median plane field versus wiggler longitudinal coordinate was also measured for a number of wiggler models and full length prototypes,[13] including both constant period length wigglers and tapered period length wigglers. An example of this, with a 4% tapered period length is given in Fig. 8. Similarly, the results for a prototype wiggler, with constant period length of 3.76 cm is also shown in Fig. 8.

For selected cases, the harmonic content of the wigglers was obtained from measured field data and was found to be acceptably small, as shown, for example in Fig. 9 for the case of a constant period wiggler, λ_o = 3.76 cm. For this case also the first and second field integral values were obtained and are given in Fig. 10. No attempt was made as yet to optimize the latter results with modification of the wiggler end field taper or "external" field correction. Further studies, including also quantitative evaluation of the "phase integral", also for the tapered prototype wiggler case, are in progress.

IV. DIELECTRIC COATED WAVEGUIDE FOR CO_2 LASER TRANSPORT

The present design of the IFEL accelerator demonstration stage transports the CO_2 laser light through a low loss rectangular waveguide with selected wall thin film dielectric coating with a theoretical loss factor[12] of $\alpha = 10^{-4}$ m^{-1}, where α is defined by $P_\ell(z) = P_\ell(0) \exp(-2\alpha z)$. A development effort has been carried on aimed at the basic mechanical design of these guides, and to carry out loss measurements and mode spectrum measurement. The elementary Zakowicz

configuration is shown in Fig. 11. Radiation wave attenuation occurs due to finite conductivity of the walls and the absorption in the dielectric coating. For $\lambda = 10$ μm, wall losses are much greater than absorption in the dielectric coating. The wall losses are proportional to $\oint_c |H_{//}|^2 d\ell$, , hence a reduction of losses is obtained with a reduction of $H_{//}$ at the wall. This, for the E-M mode of relevance here, can be done by means of a dielectric layer of thickness given by $d = (\lambda/4)(\epsilon-1)^{-1/2}$ where $\epsilon = (an_o)^2$ and an_o is the refractive index of the coating. A number of waveguide sections were constructed with internal guide cross section of 2.8 x 2.8 mm^2 and external dimensions (matched to the wiggler aperture) of 3.8 x 19.0 mm^2. The configuration is shown in Fig. 12. For the basic body of the structure, stainless steel material was used with near optical finish on the "inside" surfaces. Either dielectric coated or uncoated guide sections were used in the guide measurement procedures. For the coated case, Ge coating to a thickness of 0.65 μm on a 0.1 μm Ag coating base was used on the "vertical" walls only. Calculations using the Zakowicz model (note Fig. 12), show that the Germanium coated guides should transmit, with small attenuation, CO_2 laser radiation over distances of > 1 km, where for the uncoated stainless steel guide case the power e-folding length should be of a magnitude of $\approx$ 10 cm only.

Waveguide test pieces so constructed were used to investigate coupling into the guides, transmission loss and end mode structure. Two lasers were used for these tests. The coupling measurement made use of a pulsed CO_2 oscillator of BNL's ATF/CAP facility, set for a wavelength of 10.2 μm. The pulse duration was 100 ns, and 1% of the 100 mJ beam was used. Subsequent measurements of transmission and mode used a cw CO_2 laser (courtesy of STI Optronics) set for 10.6 μm and various output powers from 100 to 500 mW. For both lasers, a HeNe alignment laser was directed along the path of the CO_2 beam, to provide a visible reference.

In both cases, the beam was focused into the waveguide using two ZnSe lenses with 25 cm focal lengths. The lenses were mounted on a 1.2 m optical rail, in order to allow rapid adjustment of their spacing. Positions were calculated to focus the TEM_{oo} output of the lasers to a Gaussian waist with a radius ω_o between 0.8 and 1.2 mm at the entrance to the guide. These calculations were confirmed by measuring the beam profile at the location of the guide entry using a pyroelectric vidicon TV camera (Electrophysics 5400) and a digital frame grabber (Spiricon LBA-100 beam analyzer).

Measurements of mode coupling and guide attenuation are still in progress using progressively longer total guide sections. Preliminary measurement results may be summarized here, however, as follows:

* High laser power transmission, $\geq$ 80%, over lengths of guides of up to 0.8 m were measured. With individual guide sections, nominally 25 cm in length, in composite assemblies as indicated, the following power transmission values were obtained:

  SS (coupling), SS (sect.), Ge (Sect.); Transmission 90.3%
  SS (coupling), Ge (sect.), SS (Sect.); Transmission 86.1%
  SS (coupling), Ge (sect.), Ge (Sect.); Transmission 93.3%

* Low loss power transmission of the coupling section is achieved with an entrance waist of the Gaussian beam at the guide entrance set at w/B = 0.71, or w = 1.0 mm.
* Attenuation of the uncoated guide is far below the calculated e-folding length ($\approx$ 10 cm).
* For the present experimental arrangements, in general, the Germanium coated guides (Zakowicz) enhanced the power transmission by about 7%, compared with the noncoated guides.

To measure the transverse mode in the waveguide, the pyroelectric vidicon was placed 7 cm downstream from three joined sections of waveguide totaling ~ 0.8 m. A Gaussian mode was obtained with careful alignment having a maximum transmission of 86% and exit beam cross section smaller than the input beam by about a factor of 2.

As indicated, further guide development is still actively being pursued. Based on the cited preliminary results it may be concluded now that the present guide configuration, even in the uncoated execution, may be suitable for the IFEL accelerator prototype experiment. Additional work is needed (and in progress) to study the benefits of dielectric coating in longer guide lengths, relevant to a multistage accelerator sequence.

V. OPTICAL ISSUES IN THE IFEL ACCELERATOR

The use of a propagating E-M mode in a rectangular, partially dielectric coated, waveguide has been proposed by Zakowicz[12] for the IFEL accelerator, specifically for reasons of its theoretically predicted extremely low attenuation and its high efficiency in the use of laser power for the particle acceleration. As indicated above, this approach is pursued not only theoretically but also by means of extensive model development and testing.

The E-M mode adopted in the Zakowicz approach is the lowest possible mode of the low loss type. It has a sinusoidal variation of the amplitude of the component of the electric field in both transverse directions. The useful guide aperture is determined by the degree of field nonuniformity which is allowable in the accelerator operation. For example, if the amplitude seen by the beam is to be constant within 15%($\pm$7.5%), a diameter as low as 0.5 mm can be used.

Because the guide is highly "overmoded" i.e. it can support many higher order modes, both the phase and group velocity are close to the speed of light. Nevertheless, the (small) differences are important because of the tight phase tolerances with respect to the beam of electrons (phase velocity) and because of bunch length considerations (group velocity).

The relation between the propagation constant for the desired mode (k_{11}) and the free space propagation constant (k_o) is:

$$(k_{11} - k_o)/k_o = -(\pi/k_o B)^2$$

where B is the transverse dimension of the waveguide aperture. For the dimensions chosen, k_{11} differs from k_o by 2.00 x 10^{-2} radians per centimeter. To maintain a

phase accuracy of 0.1 radian, the transverse dimension must hold to a tolerance of 70 μm.

The phase velocity does not depend on the dielectric thickness (within reasonable limits) but the propagation losses do so depend. As first pointed out by Zakowicz, the losses are surprisingly insensitive to the coating thickness. Typically, a 20% change in thickness leads to a 10% increase in the (very small) power loss. If 20% is taken as a reasonable target, the .645 μm thickness must be held to about 0.1 μm. This is a relatively easy tolerance for the film deposition technology used. The group velocity can be shown to be given by:

$$v_g = c\left(1 - 2[\pi/(k_o B)^2]\right)$$

where c is the free space velocity of light. For the chosen dimensions, the second term in the bracket is 6.38×10^{-6}. For comparison, an electron of 100 MeV has a fractional difference from light velocity of 1.25×10^{-5} so in 1.0 meter the laser pulse and such an electron would "slip" by 6.5 μm.

The laser power must be introduced into the guide in a manner that efficiently transforms the diffraction limited Gaussian output beam of the high power laser into the desired low loss accelerating mode. Zakowicz analyzed this "coupling" problem in a simple overlap integral fashion. The overlap between the input beam and the field pattern of the desired mode is taken to be proportional to the coupling efficiency into that mode. Zakowicz found that this method predicted that high efficiencies (over 95%) could be obtained if the waist in the Gaussian beam was located at the waveguide aperture and if the waist size was appropriately chosen (ω/B = 0.71).

This approach, while encouraging, is approximate and also does not give any information about the transition region over which the mode becomes established. Therefore, a series of calculations have been carried out in which the actual fields in the vicinity of the coupling aperture are computed in a diffraction type of approximation. The details of these calculations will be presented elsewhere and here only the results to date are summarized.

Although the formalism permits full three dimensional calculation, so far only two dimensional studies, neglecting polarization effects, have been carried out. Nevertheless these are informative and show features which are almost certainly general. It is found that the mode pattern transforms from the input Gaussian to a stable field distribution over a distance which is comparable to the Rayleigh length of the input beam. Thus, for a Rayleigh length of 30 cm, as contemplated here, the mode pattern requires about 50 cm to stabilize.

The calculation so far ignores all losses so that the energy which goes into the other modes manifests itself as amplitude and phase noise in the propagating light. For a particular choice of waist size, the best chosen so far, it is found that after the mode has stabilized ($\approx$ 50 cm as noted above) the amplitude typically fluctuates by $\pm$ 5% and the phase by $\pm$ .05 radian.

These values are consistent with the maximum amplitude due to the other modes of 0.05 of the amplitude of the desired mode. The phase fluctuation arises because the other modes have different phase velocities from that of the desired mode. These results indicate an efficiency in coupling the power into the desired

mode of $\approx$ 90%, at least in the two dimensional case, neglecting polarization.

One important check on the calculation is given by the comparison of the phase velocity obtained from the diffraction propagation calculation and the analytic value obtained by Zakowicz. Fitting the calculated phase versus z for z = 50 cm to z = 200 cm a value of $k - k_o = 1.07 \times 10^{-2}$ is obtained. This is to be compared with 1.0×10^{-2} from the Zakowicz theory (adapted to a two dimensional case).

These results support the feasibility of efficiently coupling the laser beam into the desired mode. Further calculations are in progress to extend the studies to the full three dimensional case, to study the tolerances in waist size and alignment, and to include the effects of losses.

The above discussion is correct for the case where the metal walls can be treated as nearly (but not quite) perfect conductors and when the displacement current in the walls can be neglected. These assumptions are made at the outset in the work of Zakowicz. It was realized recently that at infra-red wavelengths these assumptions may not always be applicable and modifications to the detailed analyses may be needed. These corrections could account for the unexpectedly low attenuation of the uncoated waveguides. These modifications will be the subject of further studies.

VI. IFEL SIMULATION

A 1-D particle simulation code to model the acceleration process in a waveguide IFEL has been developed. This code incorporates in a self-consistent manner the longitudinal electron dynamics and the laser field; it also takes into account the properties of a realistic electron beam, i.e., finite radius, emittance and energy spread.

This 1-D numerical model has been used as a design tool for the demonstration stage experiment; in particular it provided the optimal tapered wiggler for the given input laser power, resonance angle and the peak wiggler field.

Subsequently, the multiparticle simulation Linac code PARMELA[14] (Phase And Radial Motion in Electron Linear Accelerators) was modified to simulate the full 3-D aspects of the IFEL interaction.

The electron orbits in a tapered linearly polarized wiggler are determined by numerically solving the relativistic Lorentz force equation. The following was included in the electron beam dynamics: a) An arbitrary initial electron distribution in "trace" space (x,x' = (dx/dz), y,y' = (dy/dz)) determined by the Twiss parameters α_x, β_x,α_y,β_y and the transverse emittances, ϵ_x and ϵ_y. b) An arbitrary longitudinal initial electron distribution in phase ϕ and energy W. c) A realistic piecewise constant tapered wiggler allowing for both horizontal and vertical focusing.

A small region of the center of the electron pulse of extent equal to the laser wavelength λ_s was modelled. Periodic boundary conditions are assumed and consequently, electrons slipping-out of the examined region are re-entered at the back.

The external laser is not a dynamical variable at this point; however, the transverse characteristics of the waveguide modes are incorporated in the simulations.

The physical model of an IFEL is described by the coupled system of equations for the i-th electron, as follows:

$$\frac{d\gamma^i}{d(ct)} = -\frac{e}{mc^2}\frac{K(x,y,z)}{2\gamma^i}[KK]\,E_0(x,y)\sin(\psi^i(z,t)+\phi_s)$$

$$\frac{d\psi^i(z,t)}{d(ct)} = \beta_z^i k_w(z) - \frac{k_s}{2\gamma^i}\Big(1+(\gamma^i\beta_x^i)^2+(\gamma^i\beta_y^i)^2 + 2K(x,y,z)\,K_s\,[KK]\cos(\psi^i(z,t)+\phi_s)\Big)$$

$$\frac{d(\gamma^i\beta_x^i)}{d(ct)} = \frac{e}{mc^2}(\beta_y^i B_z^w - \beta_z^i B_y^w)$$

$$\frac{d(\gamma^i\beta_y^i)}{d(ct)} = \frac{e}{mc^2}(\beta_z^i B_x^w - \beta_x^i B_z^w)$$

$$\frac{dx^i}{d(ct)} = \beta_x^i \qquad \frac{dy^i}{d(ct)} = \beta_y^i$$

where $E_0(x,y)$ and ϕ_s are the slowly varying laser field amplitude and phase; $K(x,y,z)$ is the wiggler constant, K_s is the corresponding laser constant and [KK] = F_1 as given in Section II. The relative phase of the electron wiggling motion to that of the laser oscillations is defined as:

$$\psi^i(z,t) = \int_o^z dz' k_w(z') + k_s z - k_s ct\ .$$

The laser field is assumed to be of the form,

$$E_s(x,y,z,t) = \overline{E}_o(x,y)\sin(k_s z - k_s ct + \phi_s) \qquad \textit{where}$$

$\overline{E}_o(x,y)$ correspond to a TM_x waveguide mode as described in Ref. [12].

A few characteristic results of the application of the 3-D simulation code to the IFEL accelerator under study are given here.

The accelerated electrons oscillate about the axis with slowly increasing amplitude ($x \approx \sqrt{\lambda_w(z)}$; the nonaccelerated electrons on the other hand have an increasing amplitude ($x \approx \lambda_W^2(z)$) and some of them wander off axis. The velocity (x') component of typical electrons in the horizontal plane is shown in Fig. 13.

The transverse phase space at the end of the wiggler is given in Fig. 14, showing some emittance growth in the horizontal plane and two well defined group of electrons (accelerated and non-accelerated) in the vertical plane with different slopes; the emittances are comparable with the initial one. The initial phase space is included for comparison.

The energy spectrum at the end of the wiggler as shown in Fig. 15, clearly illustrates the fraction of accelerated electrons ($\approx$ % 50).

Further benchmarking of the code is in progress and an extension of the code to allow for dynamical variations of the laser amplitude and phase is also contemplated.

VII. IFEL MULTISTAGE ACCELERATOR, ERROR SIMULATION

Initially the 1-D simulation code has been used to define a sequence of optimally tapered wigglers for a given input laser power, resonance phase angle and peak wiggler field; and to calculate the particle capture (bucket acceptance) and losses (bucket leakage) of a single or multistage accelerator for variation of laser power, guide loss, energy spread and wiggler errors. To this end, a basic multimodule structure 50-250 MeV IFEL accelerator was calculated, making use of a $W_L = 6.2\ 10^{11}$ Watts laser power and a multiplicity of 8 elementary, $L_{sect} = 0.6$ m, units. The parameters of this structure are detailed in Table III.

A typical phase space (γ,Ψ) at the end of the 1th and the 8th module of this multistage accelerator is given in Fig. 16. In addition to this, also the particle energy spectrum is shown, indicating the fraction of accelerated particles ($\sim$ 40%) and the fraction of unaccelerated electrons. The wiggler period $\lambda_w(z)$ as a function of distance is also given in this figure, both for the first stage and last stage of this accelerator. This piecewise constant function is inherent in a periodic tapered wiggler and reflects a realizable wiggler that best fit the smooth theoretical curve obtained self-consistently to maintain the resonance condition.

The rate of acceleration $(d\gamma/dz)$ is proportional to $\gamma^{-1/3}$, this is further emphasized in Fig. 17 where (dE/dz) and $\gamma(N)$ are given as a function of accelerator module number.

The implicit vertical transverse focussing action of the planar wiggler is taken into account. No effort has been made to shape the wiggler poles in order to achieve simultaneous horizontal transverse focussing. "External" focussing is added by means of an approximate FoDo channel, resulting in transverse optics for the 8 module accelerator as shown in Fig. 18.

A preliminary examination has been made of the sensitivity of the acceleration efficiency as a function of the laser power, loss coefficient and electron beam initial energy spread; for the case of a multistage (N = 8) accelerator. The results are shown in Fig. 19 where the 8 module accelerator net capture efficiency is shown versus resonant phase angle; in Fig. 20, where the beam capture efficiency is shown versus laser power and in Fig. 21, where the capture efficiency is shown as a function of guide attenuation coefficient α, for various laser power values. In addition, accelerator losses have been studied for the case of a wiggler with random pole-to-pole field errors. An example of this is given in Fig. 22 where the γ-Ψ plot is shown for the case of $\sigma(\Delta B_p/B_p) = 0.01$ and for the case of $\sigma(\Delta B_p/B_p = 0.05$. Clearly, the latter case is unacceptable. With the present simulation program only phase errors are considered in this case. Aspects of electron beam "walk-off" have not been taken into account, as yet. The predictions of the code have been compared with the linear theory as given in [3] and, in general, good agreement was obtained. Note that the present code has been used as a design tool for the demonstration stage experiment. It is planned now to incorporate the transverse coordinates dependence of the laser and electron beam as well as the wiggler field with the use of the 3-D program cited in the foregoing.

CONCLUDING REMARKS

The study of the IFEL accelerator is continuing with near term emphasis on low loss guide development, IFEL accelerator transverse and longitudinal phase space transport and the further parameter optimization of a multimodule $\approx$ 1 GeV accelerator.

It is evident from the foregoing IFEL accelerator parameter study that for a single demonstration stage, aimed at approximately doubling the beam energy, a CO_2 laser power of $\approx 10^{11}$ Watts is satisfactory. For a cascaded IFEL accelerator system of final energy of $\sim$ 1 GeV a laser power magnitude of $\geq 10^{12}$ Watts is required to make the overall device technically competitive.

Acknowledgement: The authors acknowledge the continuing support by the Advanced Technology R&D Branch, Division of High Energy Physics, U.S. Dept. of Energy. They also acknowledge engineering assistance from J. Sheehan, S. Ulc and M. Woodle. In addition, they wish to gratefully mention the participation in model/prototype measurements by T. Romano and J. Armendariz (wiggler) and by S. Coe and M. Weng (dielectric guides).

REFERENCES

1. R.B. Palmer, J. Appl. Phys. 43, 3014, 1972.
2. C. Pellegrini, P. Sprangle, W. Zakowicz, Intern. Conf. on High Energy Accelerators; 1983.
3. E. Courant, C. Pellegrini, W. Zakowicz, PR A, Vol. 32, No. 5, 1985.
4. E. Courant, J. Sandweiss, BNL 38915.
5. A. van Steenbergen, in Experimental Program, ATF, BNL 41664, 1988; and "IFEL Accelerator Demonstration Stage," in ATF, BNL 43702, 1989.
6. E. Courant, A. Fisher, J. Gallardo, C. Pellegrini (UCLA), J. Rogers, J. Sandweiss (Yale University), J. Sheehan, A. van Steenbergen, S. Ulc, M. Woodle, "Inverse Free Electron Laser (IFEL) Accelerator Development," ATF Users Meeting, BNL 47000, CAP 81-91P, p.235-278, October 1991; editor H.G. Kirk.
7. N. Kroll, P. Morton, M. Rosenbluth, IEEE of Quantum Electron. QE-17, 1436, 1981.
8. A. van Steenbergen, J. Gallardo, T. Romano, M. Woodle, "Fast Excitation Wiggler Development," Proc. Workshop 1 Angstrom FEL, Sag Harbor, NY, 1990, Editor J. Gallardo, p. 79, BNL 52273.
9. A. van Steenbergen, Patent Application 368618, June '89 (issued Aug. '90).
10. A. van Steenbergen, J. Gallardo, T. Romano, M. Woodle, "Fast Excitation Variable Period Wiggler," Proc. PAC San Francisco, IEEE Nucl. Sci., May 1991.
11. A. van Steenbergen, J. Gallardo, "IFEL Development, Parameterization 0.4 GeV Accelerator," Unpublished Notes, June 1990.
12. W. Zakowicz, J. Applied Physics 55, 9, 1984; also BNL 34347.
13. J. Armendariz, J. Gallardo, T. Romano, A. van Steenbergen, Fast Excitation Wiggler Field Measurement Results, BNL Report 47928 August 1992.
14. L. Young, "PARMELA", 1991 version, private communication.

Table I, Energy Dependence of Selected Parameters

$\frac{d\gamma}{dz} = \left(\frac{2}{\eta}\right)^{\frac{1}{2}} n^{\frac{1}{2}} \xi \tilde{A} \left(\frac{\lambda}{\lambda_o}\right)^{\frac{1}{2}}$	$\frac{d\gamma}{dz} = \left(\frac{2}{\eta}\right)^{\frac{1}{3}} \left(\frac{\Omega}{\omega}\right)^{\frac{1}{3}} \frac{\eta^{\frac{1}{3}}}{\gamma^{\frac{1}{3}}} \xi \tilde{A}$	$\frac{d\gamma}{dz} = \frac{K}{\gamma} \xi \tilde{A}$
Set: $\lambda_o = \lambda_o(z)$	$\left(\frac{\lambda_o}{\lambda}\right) = \left(\frac{2}{\eta}\right)^{\frac{1}{3}} \left(\frac{\Omega}{\omega}\right)^{-\frac{2}{3}} n^{\frac{1}{3}} \gamma^{\frac{2}{3}}$	$\left(\frac{\lambda_o}{\lambda}\right) = \left(\frac{2}{\eta}\right) n \frac{\gamma^2}{K^2}$
$\frac{\Omega}{\omega} = \left(\frac{2}{\eta}\right)^{\frac{1}{2}} \cdot \left(\frac{\lambda}{\lambda_o}\right)^{\frac{3}{2}} \cdot n^{\frac{1}{2}} \cdot \gamma$	set: $\Omega = \Omega(z)$	$\left(\frac{\Omega}{\omega}\right) = \left(\frac{2}{\eta}\right) \frac{K^2}{n\gamma^2}$
$K = \left(\frac{2}{\eta}\right)^{\frac{1}{2}} \left(\frac{\lambda}{\lambda_o}\right)^{\frac{1}{2}} n^{\frac{1}{2}} \cdot \gamma$	$K = \left(\frac{2}{\eta}\right)^{\frac{1}{3}} \left(\frac{\Omega}{\omega}\right)^{\frac{1}{3}} n^{\frac{1}{3}} \cdot \gamma^{\frac{2}{3}}$	set: $K = K(z)$
$a_{\frac{1}{2}} = \left(\frac{\lambda}{2\pi}\right)\left(\frac{2}{\eta}\right)^{\frac{1}{2}} \left(\frac{\lambda}{\lambda_o}\right)^{\frac{1}{2}} n^{\frac{1}{2}}$	$a_{\frac{1}{2}} = \left(\frac{2}{\eta}\right)^{\frac{2}{3}} \left(\frac{\lambda}{2\pi}\right)\left(\frac{\Omega}{\omega}\right)^{-\frac{1}{3}} n^{\frac{2}{3}} \cdot \gamma^{\frac{1}{3}}$	$a_{\frac{1}{2}} = \left(\frac{\lambda}{2\pi}\right)\left(\frac{2}{\eta}\right) \frac{n \cdot \gamma}{K}$

with: $\Omega = \frac{eB}{m_o c}$; $\omega = \frac{2\pi c}{\lambda}$; $\left(\frac{\Omega}{\omega}\right) = 93.48\lambda$ [T.m] ; $A \sin\psi = \tilde{A}$, $A = \left(\frac{e E_z}{m_o c^2}\right)$

$K = \frac{eB_o\lambda_o}{2\pi m_o c^2} = \left(\frac{\lambda_o}{\lambda}\right)\left(\frac{\gamma\lambda_o}{2\pi\rho_o}\right)$; $\rho_o = \frac{\gamma m_o c^2}{eB}$; $\left(\frac{\lambda}{\lambda_o}\right) = \frac{\eta K^2}{2n\gamma^2}$; kc = $(2\pi/\lambda)$c; $\kappa = 2\pi/\lambda_o$

$\xi_n = 1$, for a helical wiggler; $\xi_n = F_n$ for a planar wiggler n = harmonic number 1,3,5...

$F_{1,3,5} = 1/2\ [J_{0,1,2}(x) - J_{1,2,3}(x)]$; with $x = kK^2/8\kappa\gamma^2$ and J_i are Bessel functions

$\eta = 1$, helical wiggler; $\eta = 1/2$, planar wiggler

Table II, IFEL Accelerator Experiment

Electron Beam			
	Injection energy	48.9	MeV
	Exit energy	87.95	MeV
	Mean accelerating field	89	MV/m
	Current, nominal	5	mA
	N(bunch)	$6\ 10^9$	e^-
	I(max)	100	A
	$\Delta E/E$ (one σ)	$\pm 3\ 10^{-3}$	
	Emittance (one σ)	$7\ 10^{-8}$	m.rad
	Beam radius	0.3	mm
Wiggler Parameters			
	Wiggler length	0.47	m
	Section length	0.6	m
	Period length	2.86-4.32	cm
	Gap	4	mm
	Field max.(Const.B mode)	1.25	T
	Beam oscillation, $a_{1/2}$	0.17-0.22	mm
Laser Parameters			
	Power, P(laser)	$2\ 10^{11}$	Watts
	Wavelength, λ	10.2	μm
	Max.field	$1.36\ 10^3$	MV/m
	Dielectric guide, loss par. α	0.025	m^{-1}
	Field attenuation/section	0.13	dB
	Pulse length (fwhm)	6	psec

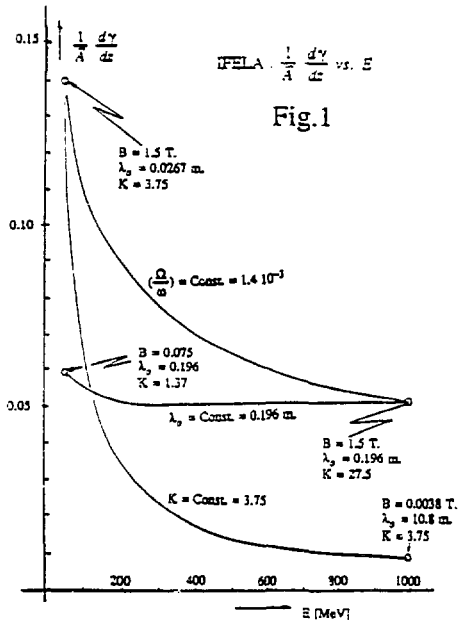

Fig.1

Fig.2

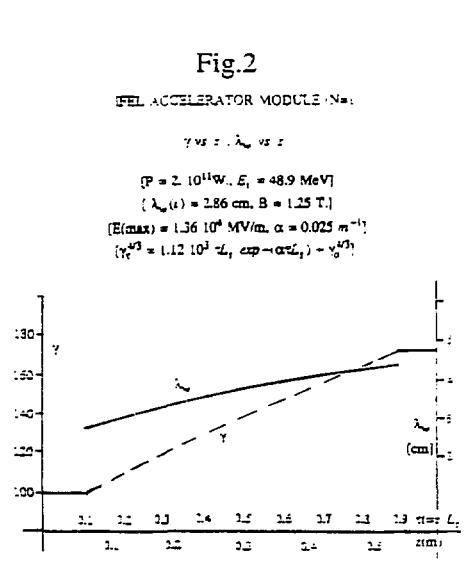

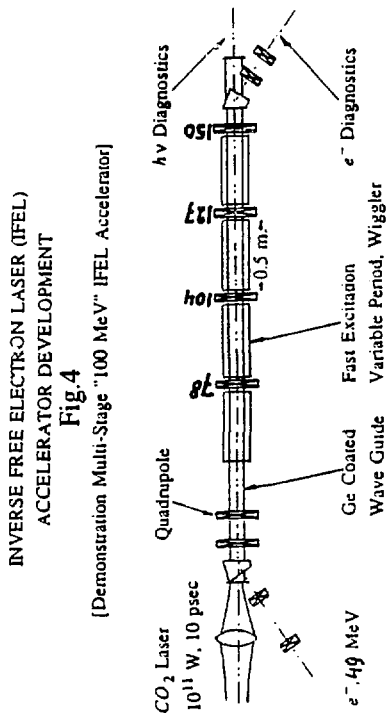

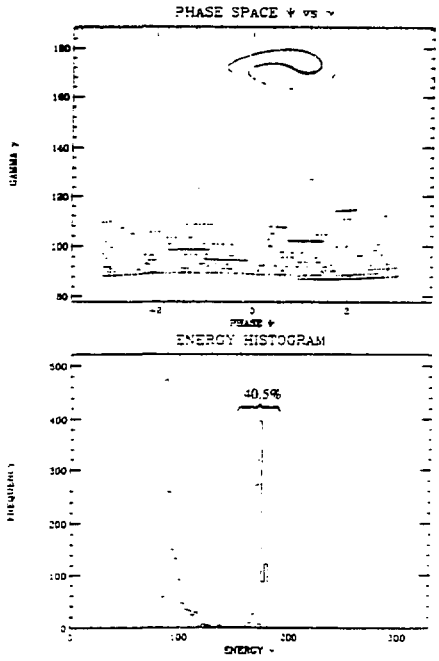

Fig.3

IFEL Accelerator Module (N=1)
P = 2.10[11] W, E = 48.9 MeV
λ_w = 2.86 cm, B = 1.25 T
E max = 1.36 10^4 MV/m, α = 0.025 m^{-1}

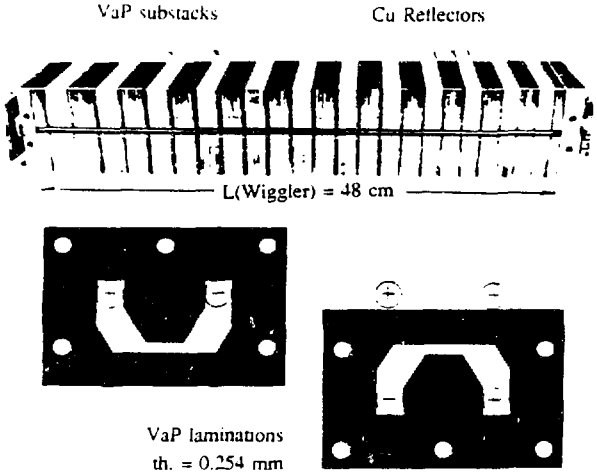

Fig.5

Fast Excitation, Variable Period, Wiggler
(IFEL Accelerator, Wiggler Prototype)
Stackable, Interleaved VaP laminations
and Cu eddy current "field reflectors"

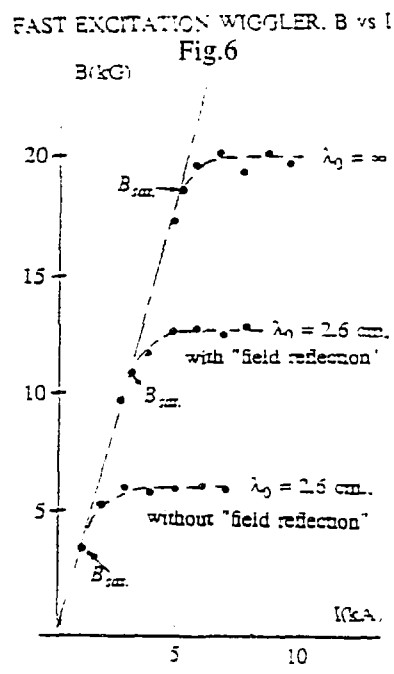

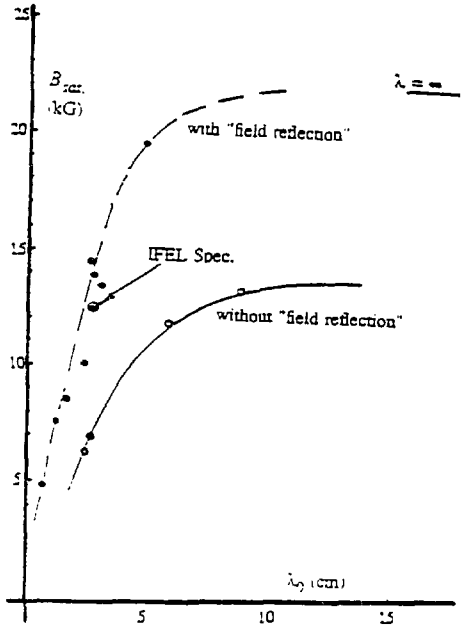

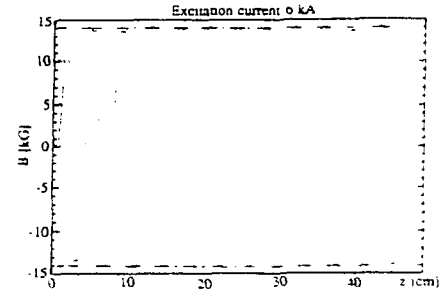

Constant Period, Fast Excitation, Wiggler
λ = 3.76 cm, g = 0.40 cm

Fig.8

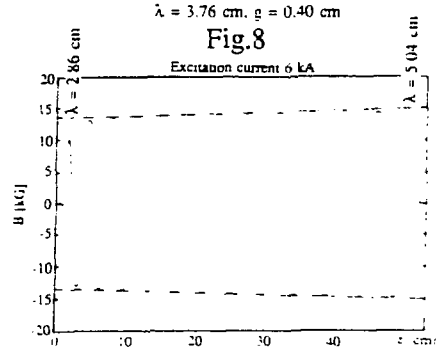

Variable Period, Fast Excitation, Wiggler
(IFEL Accelerator, Wiggler Prototype)
λ = 2.98 - 5.04 cm. g = 0.40 cm

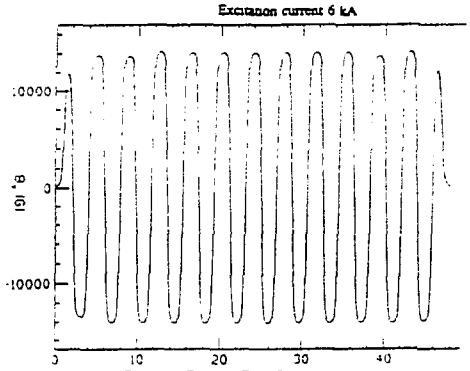

Constant Period, Fast Excitation, Wiggler
$\lambda = 3.76$ cm, $g = 0.40$ cm

Fig.9

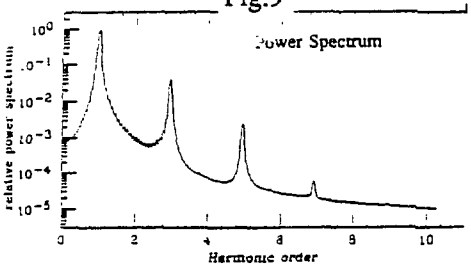

Power Spectrum, Constant Period Fast Excitation Wiggler
$\lambda = 3.76$ cm, $g = 0.40$ cm, I(exc) = 6 kA

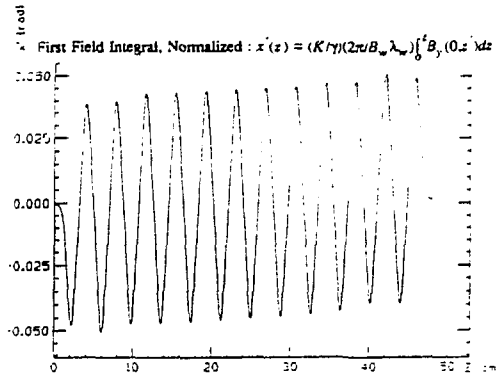

Constant Period, Fast Excitation, Wiggler
$\lambda = 3.76$ cm, $g = 0.40$ cm

Fig.10

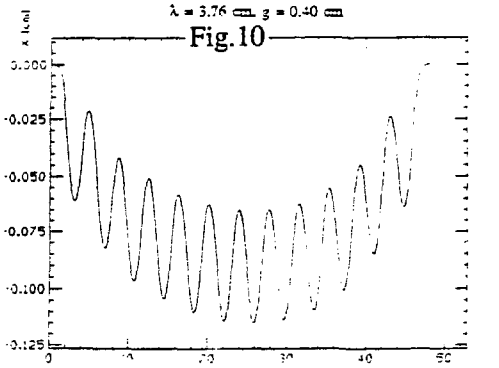

Second Field Integral, Normalized : $x = (K/\gamma)(2\pi/B_w\lambda_w)\int_0^z dz'\int_0^{z'} B_y(0,z'')dz''$

LOW LOSS DIELECTRIC COATED WAVEGUIDE
[W.Zakowicz, J.ApplPhys. 55 (9), 1984 and BNL 34347]

Fig.11

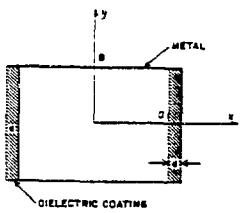

Minimum loss condition for TM_{11}^{x} hybrid mode:

$$d = (\lambda/4)(\varepsilon-1)^{-1/2}$$

where $\varepsilon = (an_0)^2$. an_0 is the refractive index of the dielectric coating.

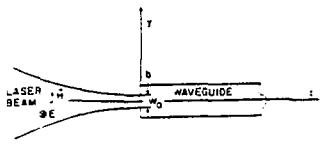

Transition Free Space - Guide Propagation

LOW LOSS DIELECTRIC COATED WAVEGUIDE

Fig.12

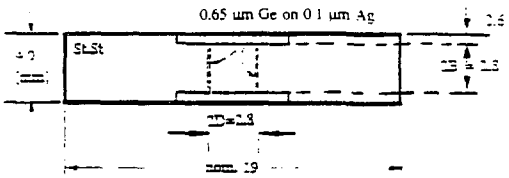

Minimum loss condition for TM_{11}^{x} hybrid mode:

$$d = (\lambda/4)(\varepsilon-1)^{-1/2}$$

where $\varepsilon = (an_0)^2$ an_0 is the refractive index of the dielectric coating

Attenuation constant α of the TM_{11}^{x} mode:

$$\alpha = \frac{c^2\pi^{3/2}}{3\omega^{3/2}\sigma^{1/2}}\left(\frac{\varepsilon^2}{\varepsilon-1}\frac{1}{B^3}+\frac{1}{B^3}\right)-\frac{\pi^3\varepsilon}{16k_0^3B^3(\varepsilon-1)^{3/2}}$$

... and B are guide dimensions, ω angular frequency, k_0 wave number in vacuum, σ wall conductivity, ε'' imag. part dielectric constant. Computed values, using $\sigma_{Cu} = 5 \cdot 10^{17}$ sec^{-1}, $\varepsilon(Ge) = 16$, $\varepsilon''(Ge) = 0.09$

$$\alpha_{tot} = \alpha_{die} = 1.6 \cdot 10^{-4} + 1.4 \cdot 10^{-3} = 1.6 \cdot 10^{-3} \quad m^{-1}$$

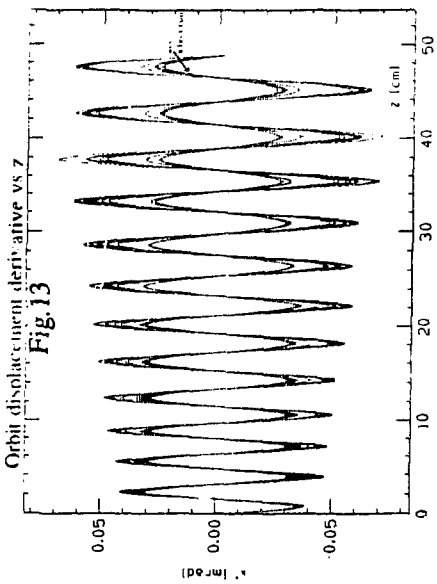

Fig.13

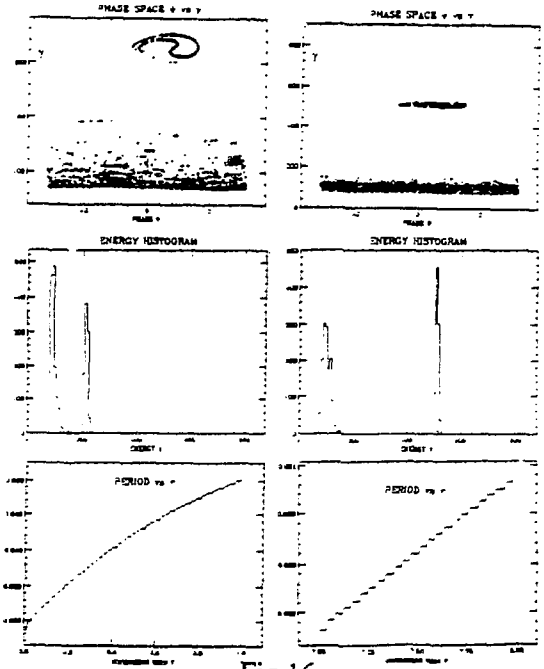

Fig.16

Example 8 Module IFEL Accelerator
("Sept.6" structure & params)

Fig.15

3-D SIMULATION, IFEL ACCELERATOR
("Sept.6 structure & parameters")
Electron Acceleration and Capture

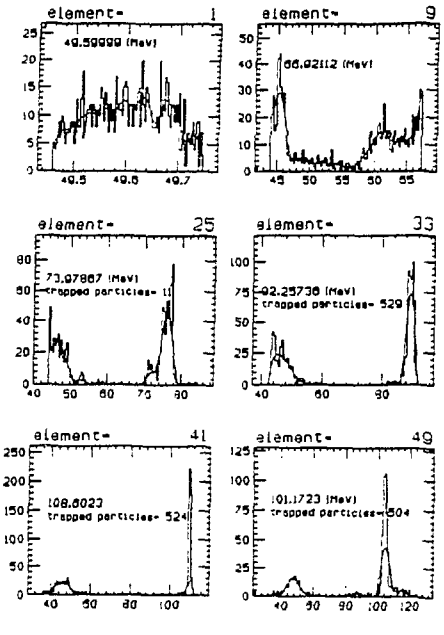

3-D SIMULATION, IFEL ACCELERATOR
("Sept.6 structure & parameters")
Evolution Transverse Phase Space, First Accel.Stage

Fig.14

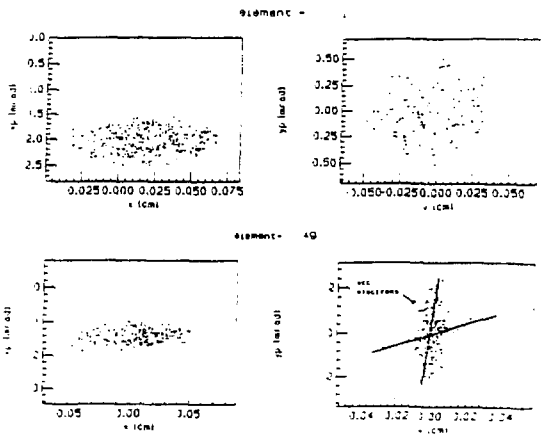

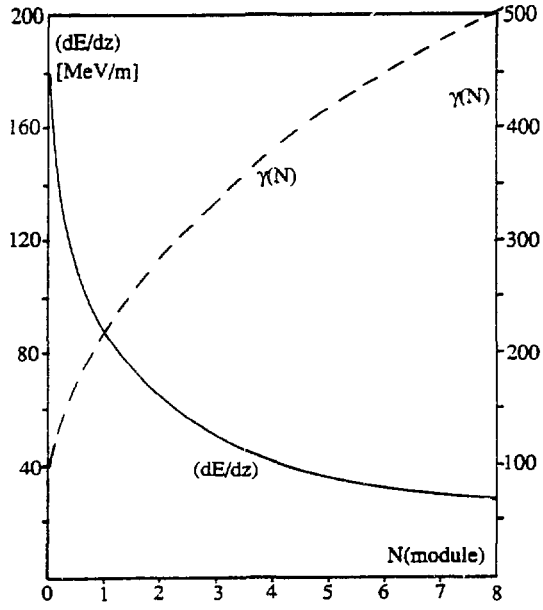

Fig.17

Example 8 Module IFEL Accelerator
("Sept.6" structure & param.s)

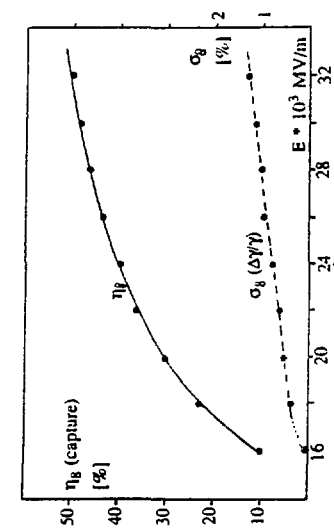

Fig.20 IFEL Linac, Beam Capture versus Laser Field
("Sept.6" structure & param.s, α = 0.025)

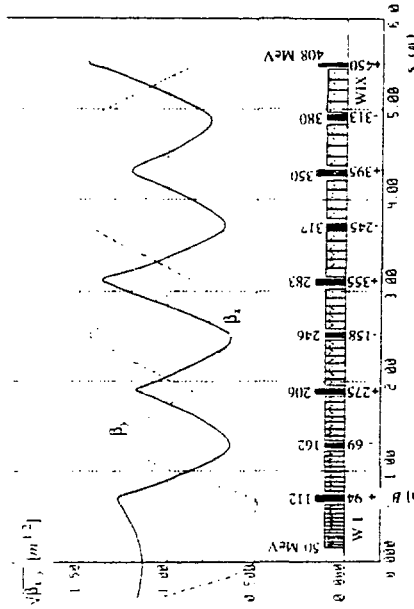

Fig.18

TRANSVERSE OPTICS FOR THE IFEL ACCELERATOR
Tapered Wiggler Modules (Vertical focusing only) in a 4G Channel
Nine Module Accelerator, P_{laser} = 5 10^{11} W, β = 0.05 m

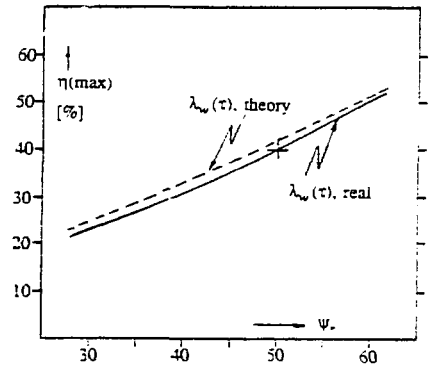

Fig.19

IFEL Accelerator, Capture Efficiency as a Function of ψ_s
("Sept.6" structure & param.s)

Fig.21

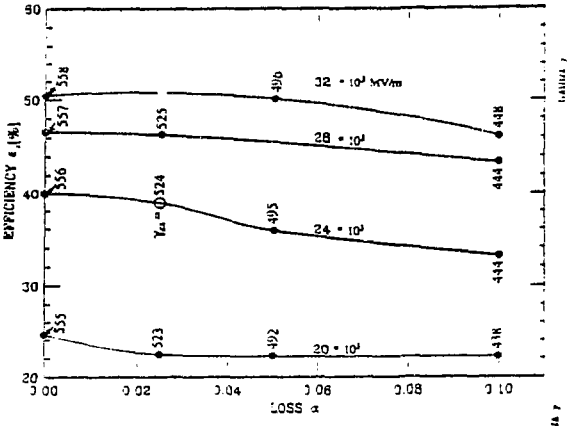

Example 8 Module IFEL Accelerator
("Sept.6" structure & param.s)

$(P_t(z) = P_t(0)\exp(-2\alpha z))$

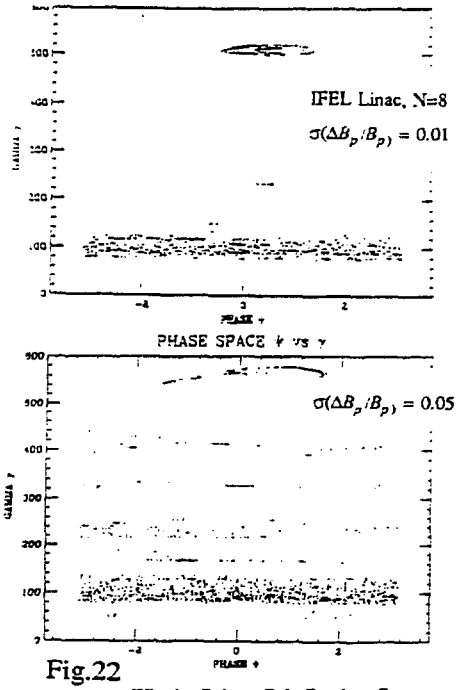

Fig.22

Wiggler Pole-to-Pole Random Errors

Table III, IFEL Multistage Accelerator

Electron Beam			Laser Parameters		
Injection energy	48.9	MeV	Power, P(laser)	6.2 10^{11}	Watts
Current, nominal	5	mA	Wavelength, λ	10.2	μm
N(bunch)	6 10^9	e^-	Max.field	2.4 10^4	MV/m
I(max)	100	A	Dielectric guide, loss α	0.025	m^{-1}
$\Delta E/E$ (one σ)	≈3 10^{-3}		Field attenuat. n/section	0.13	dB
Emittance (one σ)	7 10^{-3}	m.rad	Pulse length (fwhm)	6	psec
Beam radius	0.3	mm	Photon beam radius	0.8	mm

Accelerator: N = 8 sections; L(section) = 0.6 m.; Wiggler, constant B.

B(max) = 1.25 T.; Synchronous phase, ϕ_s = 50°, $\eta_{conv.}$ = 41%

Stage.N	L_w [m]	λ_w [cm]	Structure.n*	E(exit)[MeV]
1	0.48	2.86-5.05	23	108.56
2	0.50	5.05-6.12	17	144.28
3	0.45	6.12-6.89	13	171.50
4	0.49	6.89-7.50	13	193.33
5	0.53	7.50-7.99	13	212.32
6	0.48	7.99-8.40	11	229.35
7	0.50	8.40-8.76	11	243.94
8	0.52	8.76-9.08	11	256.94

*$L_w = [n(\lambda_w/2) - 2(\lambda_w/4)]$